Evaluation of Advanced MOSFET Threshold Voltage Drift Measurement Techniques

B. Ullmann, K. Puschkarsky, M. Waltl, H. Reisinger, and T. Grasser

***Abstract*—The experimental characterization of the threshold voltage shift in metal–oxide–semiconductor field-effect transistors due to degradation mechanisms like bias temperature instability and hot-carrier degradation requires a careful consideration of various pitfalls. One of them concerns the comparability between the threshold voltage shifts obtained by different extraction methods. The focus of this paper is set on the comparison of two extraction methods used at recovery conditions, the constant current and the constant voltage method. Although considered equivalent, a thorough experimental analysis shows that the equivalence of both methods is limited by a low device parameter change during degradation, a measurement in the sub-threshold region, and the consideration of device-to-device variability.**

***Index Terms*—Threshold voltage extraction, MSM, BTI, HCS, measurement technique, reliability.**

I. Introduction

THE PERFORMANCE of MOSFETs is affected by degradation mechanisms like bias temperature instability (BTI) and hot-carrier degradation (HCD), which are listed as the most prominent reliability challenges [1], [2]. In order to meet the reliability requirements, a correct assesment and extrapolation of the degradation is required for the design of robust circuits [3]. For this purpose, the transfer characteristics of MOSFETs are typically recorded because it provides profound insight into the degradation of device performance and allows for the development of accurate BTI and HCD models. A widely used method for the experimental characterization of MOSFET degradation is the measure-stress-measure (MSM) technique, which consists of three sequences and contains information about the stress and recovery characteristics of the degradation mechanism:

- Characterization of the virgin device, e.g., by taking an initial transfer characteristics (I_D-V_G curve).
- Stressing of the device, with a stress bias typically much higher than the nominal operating conditions.
- Post-stress characterization of the degraded device by either remeasuring an I_D-V_G characteristics or by monitoring the evolution of the threshold voltage shift ΔV_{th} at a single gate bias or drain current over a certain time period. This provides important information about the recovery of ΔV_{th} over many decades in time.

The latter allows for a more extensive analysis of the ΔV_{th} drift and makes the MSM technique quite advantageous for ΔV_{th} monitoring compared to other techniques [4], e.g., the on-the-fly (OTF) [5]. In OTF measurements drifts of ΔV_{th} are determined in a three-way measurement directly at the stress level by applying a modulation of the gate bias. This method for the back conversion of ΔI_D to ΔV_{th} requires an approximation of the I_D-V_G characteristics, which is, however, very sensitive to changes in the mobility. Due to the bias modulation the OTF method introduces a systematic error, whereas the MSM technique does not need a bias modulation. Moreover, considering a statistical error of $\pm 1\,\mathrm{mV}$ in ΔV_{th}, the relative accuracy in the measured drain current I_D needs to be 10^{-3} for the MSM technique, which is achievable with reasonable integration times, whereas 10^{-5} is required for the OTF technique [6]. A advantage of the MSM technique is the insensitivity to mobility changes induced by stress compared to the OTF technique [7]. Another advantage of the MSM technique is that it includes the information about the recovery evolution which enables the study of the permanent component of the ΔV_{th} degradation [8]. In the context of MSM measurements, two different methods are typically used to monitor ΔV_{th}.

- The constant voltage (**cv**) method: The drain current I_D is recorded at a constant voltage, typically near V_{th}. Subsequently I_D is converted to ΔV_{th} using the initial I_D-V_G curve [9].
- The constant current (**cc**) method: The threshold voltage V_{th} is monitored by recording the gate voltage controlled by a feedback loop of an operational amplifier to achieve a constant drain current [10].

A detailed review of the cv and cc method is presented in Section III. Especially for pure BTI stress, both methods have been implicitly assumed to be comparable and to provide equivalent results. However, we will show here that recovery measurements of ΔV_{th} extracted from the **cv** method

Manuscript received March 15, 2019; accepted April 5, 2019. Date of publication April 9, 2019; date of current version June 5, 2019. This work was supported in part by the Austrian Science Fund (FWF) under Project P 26382-N30, Project P 23958-N24, and Project I2606-N30, in part by the European Union FP7 Project ATHENIS 3-D under Grant 619246, and in part by the Austrian Research Promotion Agency (FFG, Take-Off Program) under Project 861022 and Project 867414. *(Corresponding author: K. Puschkarsky.)*

B. Ullmann and T. Grasser are with the Institute for Microelectronics, TU Wien, 1040 Vienna, Austria (e-mail: grasser@iue.tuwien.ac.at).

K. Puschkarsky is with the Institute for Microelectronics, TU Wien, 1040 Vienna, Austria, and also with the Reliability Department, Infineon Technologies AG, 85579 Neubiberg, Germany (e-mail: katja.puschkarsky@infineon.com).

M. Waltl is with the Institute for Microelectronics, TU Wien, 1040 Vienna, Austria, and also with the Christian Doppler Laboratory for Single-Defect Spectroscopy, TU Wien, Wien, Austria.

H. Reisinger is with the Reliability Department, Infineon Technologies AG, 85579 Neubiberg, Germany.

Color versions of one or more of the figures in this paper are available online at http://ieeexplore.ieee.org.

Digital Object Identifier 10.1109/TDMR.2019.2909993

1530-4388 © 2019 IEEE. Translations and content mining are permitted for academic research only. Personal use is also permitted, but republication/redistribution requires IEEE permission. See http://www.ieee.org/publications_standards/publications/rights/index.html for more information.

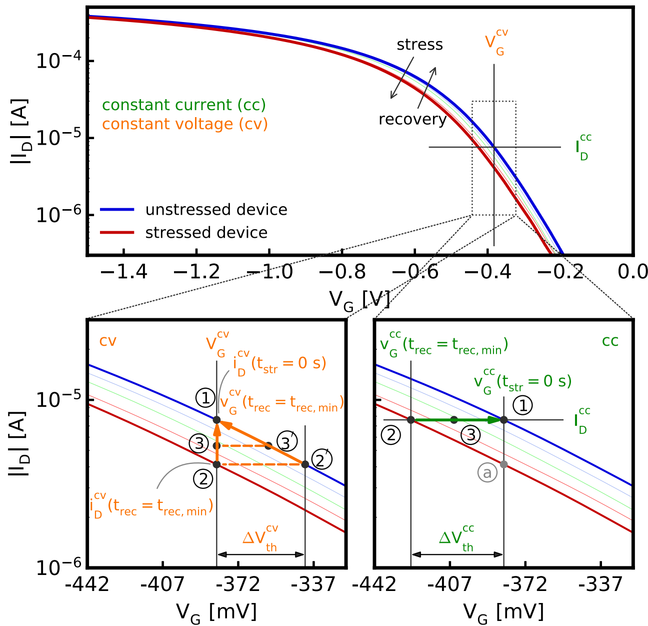

Fig. 1. I_D-V_G characteristics at V_D=−0.1 V before and after stress of a pMOSFET: **Top:** The I_D-V_G characteristics of an unstressed/stressed device (blue, red) differ due to the impact of degradation mechanisms during stress. After stress, a recovery bias is applied and the parameters recover towards their initial values (thin lines). **Bottom Left:** Constant voltage method (cv). The drain current i_D^{cv} at a constant recovery voltage V_G^{cv} is monitored. ① before stress: $i_D^{cv}(V_G^{cv}, V_D^{rec}) = i_D^{cv}(t_{str} = 0\,s)$. ② after stress: drain current is reduced to $i_D^{cv}(t_{rec} = t_{rec,min})$. ③ during recovery: $i_D^{cv}(t_{rec})$ recovers towards its initial value. Postprocessing step: $i_D^{cv}(t_{rec})$ is transformed to $v_G^{cv}(t_{rec})$. ② → ②', ③ → ③'. The threshold voltage shift can be calculated as $\Delta V_{th}^{cv}(t_{rec}) = V_G^{cv} - v_G^{cv}(t_{rec})$. **Bottom Right:** Constant current method (cc). The gate voltage v_G^{cc} is monitored while the drain current is held at I_D^{cc}. ① before stress: $v_G^{cc}(I_D^{cc}, V_D^{rec}) = v_G^{cc}(t_{str} = 0\,s)$. ② after stress: gate voltage is reduced to $v_G^{cc}(t_{rec} = 0\,s)$. ③ during recovery: $v_G^{cc}(t_{rec})$ recovers towards its initial value. The threshold voltage shift can be calculated as $\Delta V_{th}^{cc}(t_{rec}) = v_G^{cc}(t_{rec}) - v_G^{cc}(t_{str} = 0\,s)$.

and from the **cc** method recorded after HCD stress can differ significantly. These deviations might lead to inconsistent model parameters and lifetime predictions. In this work, we thoroughly analyze and discuss the difference between both measurement methods considering that MOSFET parameters like the maximum value of the transconductance $g_{m,max}$, the linear drain current $I_{D,lin}$, the saturation drain current $I_{D,sat}$ and the sub-threshold swing SS (reciprocal value of the sub-threshold slope S in a log-lin plot) are time-dependent.

As these parameters cannot be extracted from a transient ΔV_{th} trace, full I_D-V_G characteristics are required. As a consequence, depending on the selected degradation analysis method, combinations of ΔV_{th} monitoring and I_D-V_G measurements applied after BTI/HCD stress might be required. However, it has to be taken into account that such combinations introduce additional delays as during the overall MSM cycle different measurement methods have to be triggered subsequently. In addition to time delays, changes in the gate bias can accelerate and delay the recovery.

II. Experimental

Measurements are performed on Si pMOSFETs of a 130nm commercial technology with $W = 10\,\mu m$, $L = 130\,nm$, 2.2 nm nitrided gate oxide and nominal supply voltage $V_{DD} = 1.5\,V$. The wafer temperature is controlled by a thermo chuck and kept at $T = 130°C$. I_D-V_G characteristics are recorded from 21 unstressed devices with $V_D = -0.1\,V$ and $V_D = -V_{DD}$ for the linear and saturation region, respectively. The extrapolation in the linear region (ELR) method [11] is used to extract the initial threshold voltage V_{th0}. The threshold voltage is then obtained by finding the intercept of the gate voltage axis with the extrapolation of the first derivative of the I_D-V_G at its point of maximum transconductance [12]. The median initial threshold voltage for all 21 devices is $V_{th0} = (-465 \pm 10)\,mV$. Each of the 21 devices was subjected to one combination of gate and drain stress voltage ($V_D^{str} = [0, -0.5, -1, -1.5, -2, -2.5, -2.8]\,V$ and $V_G^{str} = [-1.5, -2, -2.5]\,V$) for a stress time $t_{str} = 1.1\,ks$ and subsequently ΔV_{th} is measured for a recovery time of $t_{rec,min} \approx 1\,ms$ up to $t_{rec} = 3\,ks$ with $V_D^{rec} = -0.1\,V$. Immediately after the stress, the I_D-V_G characteristics are repeated and compared to the initial I_D-V_G curves. Furthermore, the degradation of the parameters $g_{m,max}$, $I_{D,lin}$, $I_{D,sat}$ and SS is extracted for each device.

III. Extraction of the Threshold Voltage Shift

In this section, we summarize a review of the cc and cv ΔV_{th}extraction methods. Dependent on the stress conditions, the characteristic MOSFET parameters $g_{m,max}$, $I_{D,lin}$, $I_{D,sat}$, SS and V_{th} drift during stress, which can be observed comparing the initial and post-stress I_D-V_G characteristics (blue and red curve in Fig. 1). If the real permanent degradation is negligible, the MOSFET parameters would recover towards their initial values of the unstressed device during the measurement sequence and fully recover after a recovery time $t_{rec} \to \infty$. The ΔV_{th} extraction with the constant voltage and constant current method is explained in Fig. 1.

cv method (Fig. 1, bottom left):

① An initial I_D-V_G characteristics within a narrow gate bias window around the recovery voltage V_G^{cv} is measured at a recovery drain voltage V_D^{rec}, where the corresponding drain current is $i_D^{cv}(V_G^{cv}, V_D^{rec}) = i_D^{cv}(t_{str} = 0\,s)$.

② The device is subjected for the time t_{str} to stress bias (V_G^{str} with V_D^{str}) and immediately afterwards to recovery bias (V_G^{cv} and V_D^{rec}) for the time t_{rec}. As a result of the degradation during stress, directly after stress release the I_D-V_G characteristics is shifted and the drain current is reduced to $i_D^{cv}(V_G^{cv}, V_D^{rec}) = i_D^{cv}(t_{rec} = t_{rec,min})$.

③ While subjecting the device to recovery conditions the drain current recovers from its reduced value towards its initial value and is monitored simultaneously. In a post processing step, each measured value of i_D^{cv} is transformed to a voltage v_G^{cv}, which corresponds to the gate voltage at i_D^{cv} on the initial I_D-V_G characteristics (② → ②', ① → ③', ...). Finally, the threshold voltage shift can be calculated as $\Delta V_{th}^{cv}(t_{rec}) = V_G^{cv} - v_G^{cv}(t_{rec})$.

cc method (Fig. 1, bottom right):

① The gate voltage $v_G^{cc}(I_D^{cc}, V_D^{rec}) = v_G^{cc}(t_{str} = 0\,s)$ corresponding to the measurement current I_D^{cc} is obtained by

recording v_G^{cc} for a short duration at recovery conditions (drain current is held at I_D^{cc} at V_D^{rec}).

② The device is subjected to a stress bias (V_G^{str} and V_D^{str}) for the time t_{str} and subsequently to the recovery bias V_D^{rec} while the drain current is held at I_D^{cc} for the time t_{rec}. Due to the device degradation during stress, the measured gate voltage is reduced $v_G^{cc}(I_D^{cc}, V_D^{rec}) = v_G^{cc}(t_{rec} = t_{rec,min})$.

③ During recovery, the measured gate voltage recovers towards its initial value and is monitored simultaneously. The ΔV_{th} obtained using the cc method does not require a transformation, ΔV_{th} can be calculated directly for all v_G^{cc}: $\Delta V_{th}^{cc}(t_{rec}) = v_G^{cc}(t_{rec}) - v_G^{cc}(t_{str} = 0\,s)$.

We extract the ΔV_{th}^{cv} and ΔV_{th}^{cc} in two regions: Near V_{th0} of the initial curve (sub-threshold region, abbreviated with sub in the following) and above the threshold voltage. It has to be noted that these extractions correspond to a certain device degradation level and do not consider the evolution of the parameters during recovery.

Both methods can only be considered equivalent if the following requirements are met: The I_D-V_G characteristics shifts parallel along the V_G-axis during stress and recovery, which means that the slope and curvature between ① and ②' in the left bottom sub-figure of Fig. 1 equals the shape of the curve section between ② and ⓐ in the right bottom sub-figure. In other words, $g_{m,max}$ and SS do not change significantly during the experiment. Furthermore, the device-to-device parameter variations (variability) have to be considered properly. In fact, all MOSFET parameters drift differently during stress and recovery, strongly depending on the stress conditions. As a result, the shapes of the unstressed and stressed I_D-V_G curve differ from each other, which leads to $\Delta V_{th}^{cc} \neq \Delta V_{th}^{cv}$ as discussed in the next section.

IV. Results and Discussion

We now analyze and discuss the difference between both measurement methods. Measurements were performed with 21 devices, each of them subjected to different V_G^{str}-V_D^{str} combinations, which corresponds to different HCS and BTI contributions. The relative difference between the two measurement methods is calculated as:

$$\delta = (\Delta V_{th}^{cc} - \Delta V_{th}^{cv})/\Delta V_{th}^{cc} \cdot 100\ [\%] \quad (1)$$

In the following, we distinguish the two extraction cases, illustrated in Fig. 2: Consideration of device variability and no consideration of device variability.

In the first case, the recovery conditions are set with the same spacing to V_{th0} for each device (Fig. 2 top). This means that V_G^{cv} or I_D^{cc} must be selected individually, depending on V_{th0}. In our measurements, we define the recovery conditions as $V_G^{cv} = V_{th0} + 35\,mV$ or $I_D^{cc} = I_D(V_{th0} + 35\,mV)$ for the sub-threshold region and $V_G^{cv} = V_{th0} - 130\,mV$ or $I_D^{cc} = I_D(V_{th0} - 130\,mV)$ for the region above V_{th0}, both at V_D^{rec}. This ensures that the measurement current in the cc method corresponds to the measurement voltage in the cv method. Therefore, all MOSFETs are measured at equivalent recovery conditions.

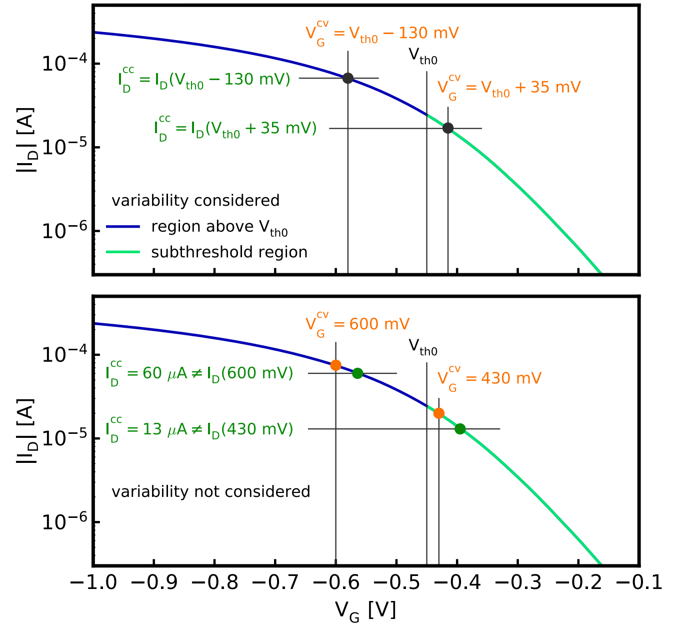

Fig. 2. Recovery conditions for constant voltage and constant current method: I_D-V_G characteristics for one device at V_D^{rec} **Top:** Variability is considered as the recovery conditions are chosen in equidistant intervals to V_{th0} for each device individually. This ensures that the measurement current for the cc method corresponds always to the measurement voltage in the cv method. **Bottom:** Variability is not considered as the recovery conditions are fixed for every device so that on average $I_D^{cc} = I_D(V_G^{cv})$.

In the second case, by contrast, the recovery conditions are set to fixed values, independent from the individual V_{th0} (for these measurements: $V_G^{cv} = -0.43\,V$ or $I_D^{cc} = -13\,\mu A$ in the sub-threshold region and $V_G^{cv} = -0.6\,V$ or $I_D^{cc} = -60\,\mu A$ in the region above V_{th0}). On average, the requirement $I_D^{cc} = I_D(V_G^{cv})$ is met, but this does not hold for every device as shown in Fig. 2 on the bottom. An analysis is required before the stress experiments in order to determine the average I_D-V_G characteristics and define the recovery conditions. However, it has to be noted that if V_G^{cv} and I_D^{cc} correspond to different recovery conditions, this can lead to different ΔV_{th} even after the same stress as discussed in [13]. Thus, the calculated δ between the measurement methods includes device-to-device variations like all other device parameter (approximately 2%). By contrast, the consideration of variability requires an I_D-V_G analysis per device prior to each experiment, therefore a deviation in $|\delta|$ due to variability is prevented. Nevertheless, even when considering variability $|\delta| > 0$ as discussed in the following. In Fig. 3 the relative difference δ of both extraction methods is shown for the relative degradation of $g_{m,max}$, $I_{D,lin}$, $I_{D,sat}$ and SS. Variability is considered and δ is shown for two regions of the I_D-V_G characteristics: above threshold (magenta) and sub-threshold (blue). Each point in the scatter plot corresponds to the measurement of one single device, which has been subjected to a certain V_G^{str}-V_D^{str} combination. This leads to different $\Delta g_{m,max}$, $\Delta I_{D,lin}$, $\Delta I_{D,sat}$ and ΔSS for each device. It has to be noted that the degradation of ΔSS is negative because the sub-threshold swing increases while all other parameters decrease with stress. Additionally, in order to analyze if δ correlates with the degradation of the MOSFET

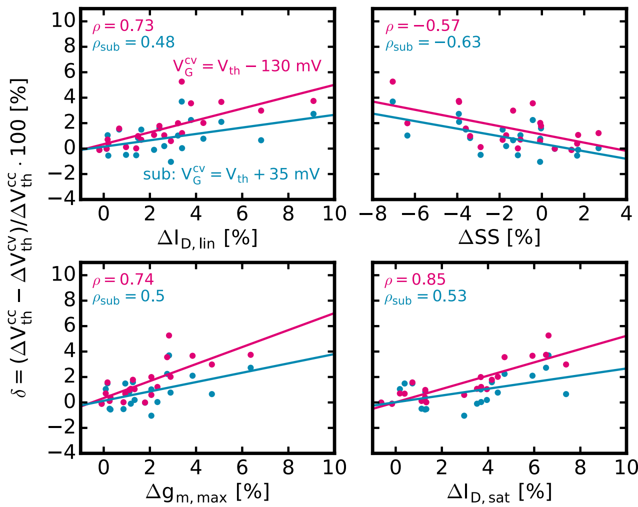

Fig. 3. Correlation of $\boldsymbol{\delta}$ with the degradation of MOSFET parameters under consideration of device variability: The parameters for each point in the scatter plots are extracted from one measurement with a certain $V_{\mathrm{G}}^{\mathrm{str}}$-$V_{\mathrm{D}}^{\mathrm{str}}$ combination of ($V_{\mathrm{D}}^{\mathrm{str}} = [0, -0.5, -1, -1.5, -2, -2.5, -2.8]$ V and $V_{\mathrm{G}}^{\mathrm{str}} = [-1.5, -2, -2.5]$ V) for $t_{\mathrm{str}} = 1.1$ ks. δ is determined from two regions of the I_{D}-V_{G} characteristics: the sub-threshold region (blue) and above the threshold voltage (magenta). For both regions, the Pearson correlation coefficient ρ_{sub} and ρ is given. The lines indicate the linear regression for each region. δ increases with larger degradation and it is on average lower for the sub-threshold region.

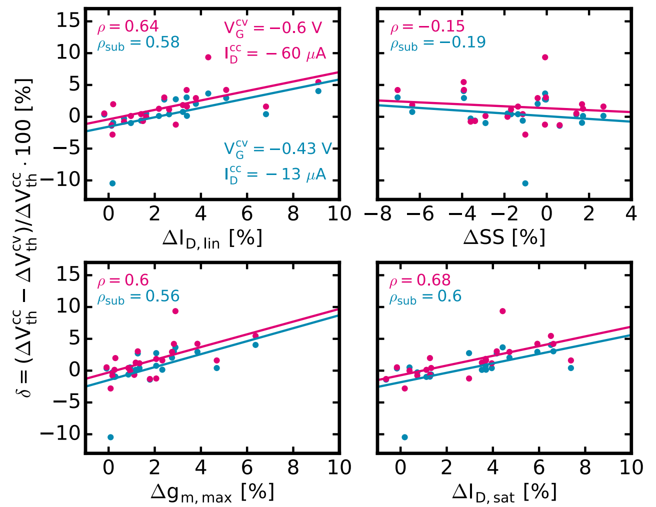

Fig. 4. Correlation of $\boldsymbol{\delta}$ with the degradation of MOSFET parameters not considering device variability: Similar to the conclusions from Fig. 3. Here, $v_{\mathrm{G}}^{\mathrm{cc}}(t_{\mathrm{str}} = 0\,\mathrm{s}) \neq V_{\mathrm{G}}^{\mathrm{cv}}$, introduces device-to-device variations of δ, which is independent from device degradation after stress and explains the weaker correlation and outliers even at low degradation.

parameters, the Pearson correlation coefficient as a measure for linear correlation between δ and $\Delta g_{\mathrm{m,max}}$, $\Delta I_{\mathrm{D,lin}}$, $\Delta I_{\mathrm{D,sat}}$ and ΔSS is given for each region: ρ_{sub} for the sub-threshold region and ρ for measurements performed above V_{th0}. δ correlates differently with the relative change of the MOSFET parameters and it can be seen in Fig. 3 that

- On average δ increases with larger degradation of $g_{\mathrm{m,max}}$, $I_{\mathrm{D,lin}}$, $I_{\mathrm{D,sat}}$ and SS for both regions.
- δ is lower for the sub-threshold region.
- The maximum difference is $\delta_{\max} < 6\%$.
- δ correlates strongly with ΔSS determined in the sub-threshold region but weakly in the region above V_{th0}.
- δ correlates strongly with $\Delta g_{\mathrm{m,max}}$, $\Delta I_{\mathrm{D,lin}}$, $\Delta I_{\mathrm{D,sat}}$ determined in the region above V_{th0}, but not so strongly in the sub-threshold region.

The correlation between δ and ΔSS, $\Delta g_{\mathrm{m,max}}$, $\Delta I_{\mathrm{D,lin}}$, and $\Delta I_{\mathrm{D,sat}}$ is dominated by the impact of the MOSFET parameter shift on the change of the slope and the curvature of the I_{D}-V_{G} characteristics. This means that the shapes of the section between ① and ②' in the left bottom sub-figure of Fig. 1 and the section between ② and ⓐ in the right bottom sub-figure of Fig. 1 differ. For example, $|\Delta g_{\mathrm{m,max}}| > 0$ or $|\Delta SS| > 0$ results in $|\delta| > 0$. While SS characterizes essentially the slope and the curvature in the sub-threshold region, $\Delta g_{\mathrm{m,max}}$, $\Delta I_{\mathrm{D,lin}}$ and $\Delta I_{\mathrm{D,sat}}$ affect the slope and curvature at $V_{\mathrm{th0}} - 130$ mV. Thus, a change of SS during stress and recovery affects mainly δ in the sub-threshold region. However, the analysis shows that δ does not exceed 4% if the measurement point is selected in the sub-threshold region.

In Fig. 4 the extraction of the parameters is performed with the measurement points at fixed values near the mean value of V_{th0}. Thus, the variability of the MOSFETs is not considered. Still as for the consideration of device variability in Fig. 3, the relative difference between the two measurement methods δ increases with larger degradation and δ is on average lower for the sub-threshold region. However, the maximum difference is higher, $\delta_{\max} > 10\%$. Furthermore, the correlation coefficients ρ_{sub}, ρ are smaller. In this case $V_{\mathrm{G}}^{\mathrm{cv}}$ does not correspond to $I_{\mathrm{D}}^{\mathrm{cc}}$. $\Delta V_{\mathrm{th}}^{\mathrm{cv}}$ and $\Delta V_{\mathrm{th}}^{\mathrm{cc}}$ are extracted for different recovery conditions. As mentioned, this introduces device-to-device variations of δ, which are independent of device degradation after stress and explains the weaker correlation and additional measurement differences even at low degradation.

Measurements of the recovery of ΔV_{th} confirm these results: For low degradation of the parameters (ΔSS, $\Delta g_{\mathrm{m,max}}$, $\Delta I_{\mathrm{D,lin}}$, and $\Delta I_{\mathrm{D,sat}} \leq 2\%$), the cc method and the cv method show quite comparable results (e.g., pure BTI stress). On the contrary, for degradation caused by a mixture of BTI and HCD or pure HCD, where the parameter degradation exceeds 4%, completely different ΔV_{th} traces are measured for the cc and cv method as shown in Fig. 5. The difference δ in the measurement methods is $\approx -10\%$ at short recovery times $t_{\mathrm{rec}} < 10^{-2}$ s, but increases with t_{rec}. Fig. 5 shows that the evolution of the slope and the curvature during the measure sequence can differ significantly. For example, if $\Delta g_{\mathrm{m,max}}$ does not recover but ΔV_{th} does, the shape of the I_{D}-V_{G} characteristics distorts during the measure sequence. The transconductance can reduce due to stress because of increased scattering with charged interface states. The decrease strongly depends on the stress conditions [14]–[16].

From this analysis it cannot be concluded which of both techniques should be considered for ΔV_{th} measurements. Nevertheless, we now briefly discuss the advantages and disadvantages of both measurement methods. The constant voltage setup as used in [17], [18] measures the drain current with a transimpedance amplifier where the feedback resistor defines the measurement range for I_{D} during stress as well as during the measure sequence. Since I_{D} can vary between the stress

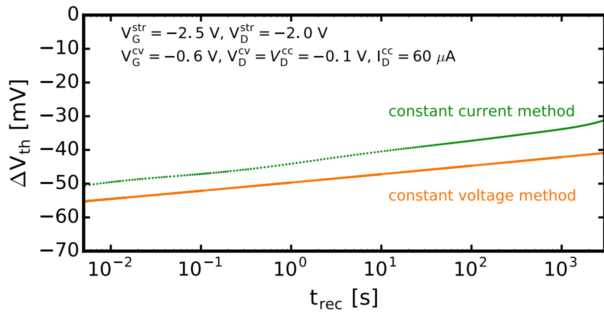

Fig. 5. Recovery traces of the threshold voltage shift monitored with the cv and cc method: Degradation caused by a mixture of BTI and HCD lead to different evolution of the ΔV_{th} recovery.

and measure sequence by a few orders of magnitude, to ensure a proper measurement resolution during the measurement, the feedback resistor has to be changed between stress and recovery. Thus, an additional delay on the order of milliseconds is typically introduced and important ΔV_{th} evolution information during the first milliseconds after stress cannot be measured. Furthermore, a requirement for the proper choice of the feedback resistor is the estimation of the degradation of the device prior to the MSM measurement. By contrast, the cc setup as proposed in [10] minimizes the delay between stress and measure sequence, because no feedback resistor has to be changed between both sequences. Consequently, the cc method is also advantageous in the case that the degradation of the device cannot be estimated prior to the MSM measurement. Another measurement requirement is a constant stress voltage applied to the gate, to avoid changes of the state of degradation. This is easier to implement for the cv method because the MSM sequences can be realized with one voltage source. This is not the case for the cc method where a voltage source is required during stress and a current source is required during recovery (also discussed in [6]).

The parameters, which define the shape of the I_D-V_G characteristics (V_{th}, SS, $g_{m,max}$, $I_{D,lin}$, $I_{D,sat}$) shift very differently during stress and recovery. This leads to significant differences in the ΔV_{th}^{cc} and ΔV_{th}^{cv} recovery behavior after particular stress conditions. A widely used analysis is fitting a power-law to ΔV_{th}. Due to the different recovery for the cv and cc method, this leads to different power-law fitting parameters, which is not physical. Thus, in order to describe degradation mechanisms properly, the impact of degradation mechanisms on all parameters has to be taken into account. Furthermore, the used measurement method and its effect on the measured parameters has to be considered in the model. If these requirements are met, the difference of both measurement methods is of secondary importance.

V. Conclusion

The extraction of ΔV_{th} using a constant current or constant voltage method in MSM sequences are equivalent if three requirements are fulfilled: First, the I_D-V_G characteristics shift during stress and measurement along the V_G-axis but does not change its slope and curvature significantly. Second, the measurement current in the cc method and the measurement voltage in the cv method are chosen in the sub-threshold region close to V_{th0}. Third, device to device variability is taken into account, which means that the recovery conditions are set individually for each device depending on its initial threshold voltage. In case that one of these requirements is not met and depending on the stress and measurement conditions, the extracted ΔV_{th}^{cc} and ΔV_{th}^{cv} can even differ by more than 10%.

References

[1] Semiconductor Industry Association. *2015 International Technology Roadmap for Semiconductors (ITRS)*. Accessed: Jun. 5, 2015. [Online]. Available: https://www.semiconductors.org/wp-content/uploads/2018/06/5_2015-ITRS-2.0_More-Moore.pdf

[2] J. H. Stathis, "The physics of NBTI: What do we really know?" in *Proc. IEEE Int. Rel. Phys. Symp. (IRPS)*, Burlingame, CA, USA, 2018, pp. 1–4.

[3] C. Schlünder, "Device reliability challenges for modern semiconductor circuit design—A review," *Adv. Radio Sci.*, vol. 7, pp. 201–211, May 2009.

[4] V. Putcha *et al.*, "Design and simulation of on-chip circuits for parallel characterization of ultrascaled transistors for BTI reliability," in *Proc. IEEE Int. Integr. Rel. Workshop Final Rep. (IIRW)*, 2014, pp. 99–102.

[5] M. Denais *et al.*, "On-the-fly characterization of NBTI in ultra-thin gate oxide PMOSFETs," in *Proc. Int. Electron Devices Meeting (IEDM)*, Dec. 2004, pp. 109–112.

[6] H. Reisinger, U. Brunner, W. Heinrigs, W. Gustin, and C. Schlünder, "A comparison of fast methods for measuring NBTI degradation," *IEEE Trans. Device Mater. Rel.*, vol. 7, no. 4, pp. 531–539, Dec. 2007.

[7] T. Grasser, P.-J. Wagner, P. Hehenberger, W. Goes, and B. Kaczer, "A rigorous study of measurement techniques for negative bias temperature instability," *IEEE Trans. Device Mater. Rel.*, vol. 8, no. 3, pp. 526–535, Sep. 2008.

[8] T. Grasser *et al.*, "The 'permanent' component of NBTI: Composition and annealing," in *Proc. Int. Rel. Phys. Symp.*, Monterey, CA, USA, Apr. 2011, pp. 6A.2.1–6A.2.9.

[9] B. Kaczer *et al.*, "Ubiquitous relaxation in BTI stressing—New evaluation and insights," in *Proc. Int. Rel. Phys. Symp. (IRPS)*, Apr. 2008, pp. 20–27.

[10] H. Reisinger *et al.*, "Analysis of NBTI degradation-and recovery-behavior based on ultra fast VT-measurements," in *Proc. Int. Rel. Phys. Symp. (IRPS)*, San Jose, CA, USA, Mar. 2006, pp. 448–453.

[11] A. Ortiz-Conde *et al.*, "A review of recent MOSFET threshold voltage extraction methods," *Microelectron. Rel.*, vol. 42, pp. 583–596, Apr./May 2002.

[12] A. Ortiz-Conde *et al.*, "Revisiting MOSFET threshold voltage extraction methods," *Microelectron. Rel.*, vol. 53, no. 1, pp. 90–104, 2013.

[13] T. Grasser *et al.*, "The paradigm shift in understanding the bias temperature instability: From reaction–diffusion to switching oxide traps," *IEEE Trans. Electron Devices*, vol. 58, no. 11, pp. 3652–3666, Nov. 2011.

[14] A. Bravaix and V. Huard, "Hot-carrier degradation issues in advanced CMOS nodes," in *Proc. Eur. Symp. Rel. Electron Devices (ESREF) Tut.*, 2010, pp. 1267–1272.

[15] S. Rauch and G. L. Rosa, "CMOS hot carrier: From physics to end of life projections, and qualification," in *Proc. Int. Rel. Phys. Symp. (IRPS) Tut.*, 2010, pp. 1–15.

[16] S. E. Tyaginov *et al.*, "Interface traps density-of-states as a vital component for hot-carrier degradation modeling," *Microelectron. Rel.*, vol. 50, nos. 9–11, pp. 1267–1272, 2010.

[17] T. Grasser *et al.*, "The time dependent defect spectroscopy (TDDS) for the characterization of the bias temperature instability," in *Proc. Int. Rel. Phys. Symp. (IRPS)*, Anaheim, CA, USA, May 2010, pp. 16–25.

[18] T. Grasser, "Stochastic charge trapping in oxides: From random telegraph noise to bias temperature instabilities," *Microelectron. Rel.*, vol. 52, no. 1, pp. 39–70, 2012.